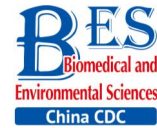


Original Article



Protective Effect of Angiotensin (1-7) on Silicotic Fibrosis in Rats*

ZHANG Bo Nan^{1,2,3}, XU Hong², GAO Xue Min⁴, ZHANG Gui Zhen^{2,3}, ZHANG Xin², and YANG Fang^{2,#}

1. School of Public Health, North China University of Science and Technology, Tangshan 063210, Hebei, China; 2. Hebei Key Laboratory for Organ Fibrosis, Medical Research Center, North China University of Science and Technology, Tangshan 063210, Hebei, China; 3. Hebei Key Laboratory for Chronic Diseases, Tangshan Key Laboratory for Clinical and Basic Research on Chronic Diseases, School of Basic Medical Sciences, North China University of Science and Technology, Tangshan 063210, Hebei, China; 4. Basic Medical College, Hebei Medical University, Shijiazhuang 050017, Hebei, China

Abstract

Objective Silicosis, caused by inhalation of silica dust, is the most serious occupational disease in China and the aim of present study was to explore the protective effect of Ang (1-7) on silicotic fibrosis and myofibroblast differentiation induced by Ang II.

Methods HOPE-MED 8050 exposure control apparatus was used to establish the rat silicosis model. Pathological changes and collagen deposition of the lung tissue were examined by H.E. and VG staining, respectively. The localizations of ACE2 and α -smooth muscle actin (α -SMA) in the lung were detected by immunohistochemistry. Expression levels of collagen type I, α -SMA, ACE2, and Mas in the lung tissue and fibroblasts were examined by western blot. Levels of ACE2, Ang (1-7), and Ang II in serum were determined by ELISA. Co-localization of ACE2 and α -SMA in fibroblasts was detected by immunofluorescence.

Results Ang (1-7) induced pathological changes and enhanced collagen deposition *in vivo*. Ang (1-7) decreased the expressions of collagen type I and α -SMA and increased the expressions of ACE2 and Mas in the silicotic rat lung tissue and fibroblasts stimulated by Ang II. Ang (1-7) increased the levels of ACE2 and Ang (1-7) and decreased the level of Ang II in silicotic rat serum. A779 enhanced the protective effect of Ang (1-7) in fibroblasts stimulated by Ang II.

Conclusion Ang (1-7) exerted protective effect on silicotic fibrosis and myofibroblast differentiation induced by Ang II by regulating ACE2-Ang (1-7)-Mas axis.

Key words: Silicosis; Ang II; Myofibroblasts; Ang (1-7); A779

Biomed Environ Sci, 2019; 32(6): 419-426

doi: 10.3967/bes2019.057

ISSN: 0895-3988

www.besjournal.com (full text)

CN: 11-2816/Q

Copyright ©2019 by China CDC

INTRODUCTION

Silicosis, caused by long-term inhalation of free silica dust, is a major occupational disease worldwide, especially in

developing countries^[1,2]. Formation of silicotic nodules and diffused pulmonary fibrosis exhibit the characteristic pathological changes of silicosis^[3]. It has been previously reported that renin-angiotensin system (RAS) plays an important role in the

*This study was supported by the National Natural Science Foundation of China [grant no. 81472953]; Natural Science Foundation of Hebei Province [grant no. H2016209170]; Graduate Student Innovation Fund of Hebei Province [grant no. 2016196]; Graduate Student Innovation Fund of North China University of Science and Technology [grant no. 2016B10]; and undergraduate innovative project of North China University of Science and Technology [grant no. X2017354].

#Correspondence should be addressed to YANG Fang, Professor, Doctor, Tel: 86-315-8805522, E-mail: fangyang_1955@126.com

Biographical note of the first author: ZHANG Bo Nan, male, born in 1982, Lecture, Master, majoring in mechanism and prevention of silicosis.

pathogenesis of hypertension, renal injury, cardiovascular disease, and pulmonary fibrosis^[4-6]. Angiotensinogen (AGT) was produced by liver and converted to angiotensin I by rennin, which is expressed in juxtaglomerular apparatus of kidney, followed by a second transformation to angiotensin II (Ang II) catalyzed by angiotensin converting enzyme (ACE) on the surface of the lung endothelium^[7]. Previous studies have indicated that the levels of ACE and Ang II increase in the serum of silicotic patient^[8]. The expressions of ACE, Ang II, and Ang II type 1 receptor (AT1) are also upregulated in the lung tissue of silicotic rats^[9]. ACE-Ang II-AT1 axis exerts important regulatory role during silicosis and inhibits the development of silicosis by blocking the activation of ACE-Ang II-AT1 axis^[10]. ACE2-Ang (1-7)-Mas, another important target axis of RAS, exhibits opposite action on ACE-Ang II-AT1 axis. ACE2 can hydrolyze Ang II to Ang (1-7) and exert anti-pulmonary fibrosis effect by binding with Mas^[11]. Ang (1-7) or overexpression of ACE2 can inhibit the pulmonary fibrosis induced by bleomycin. A779, a Mas receptor inhibitor, can attenuate the anti-fibrotic effect of Ang (1-7)^[12]. ACE2-Ang (1-7)-Mas axis is closely related to organ fibrosis and whether it also participates in the pathogenesis of silicosis is still unknown. In the present study, we explored the role of ACE2-Ang (1-7)-Mas axis and protective effect of Ang (1-7) on the rat silicosis model and myofibroblast differentiation induced by Ang II to elucidate the pathogenic mechanisms and identify novel therapeutic targets of silicosis.

MATERIALS AND METHODS

Experimental Animals and Establishment of Silicosis Model

The animal experiment protocol was approved by North China University of Science and Technology experimental animal ethics committee. The study was carried out in accordance with the guidelines of the Declaration of Helsinki. Thirty specific pathogen-free male Wistar rats (3 weeks of age) were obtained from Vital River Laboratory Animal Technology Co. Ltd. (SCXK 2009-0004, Beijing, China). The rats were housed in a temperature-controlled facility (25 ± 1 °C, $55\% \pm 10\%$ humidity) with a 12 h light/dark cycle and *ad libitum* supply of food and water regularly. HOPE-MED 8050 exposure control apparatus supplied by HOPE Industry and Trade Co. Ltd. (Tianjin, China) was used to establish the silicosis

model. This system can be set to a certain dust concentration and it is a non-invasive instrument for allowing animal inhalation. The parameters were set as follows: exposure chamber volume, 0.3 m^3 ; cabinet temperature, 20-25 °C; humidity, 70%-75%; pressure, -50 Pa to +50 Pa; oxygen concentration, 20%; flow rate of SiO₂ (5 μm silica particles; s5631, Sigma-Aldrich, USA), 3.0-3.5 mL/min; dust mass concentration in the cabinet, $2,000 \text{ mg/m}^3$. The rats were randomly divided into three groups ($n = 10$) as follows, 1) 24 weeks control group (treated with 0.9% saline from week 16); 2) 24 weeks silicosis group (inhalation of SiO₂ for 24 weeks and treated with 0.9% saline from week 16); 3) Ang (1-7) treatment group [inhalation of SiO₂ for 24 weeks and treated with Ang (1-7) from week 16]. The animal inhaled SiO₂ for 3 h per day. Ang (1-7) [$24 \mu\text{g}/(\text{kg}\cdot\text{h})$; H-1715, Bachem, USA] and 0.9% saline were administered *via* a mini-osmotic pump (200 μL; Alzet, Durect, USA) implanted into the abdominal cavity^[12,13]. The mini-pump delivered Ang (1-7) at an average flow rate of 2.5 μL/h for 30 days. Then, it is replaced by another pump in abdominal cavity. The compound was absorbed into the blood *via* omentum. The rats in each group were anesthetized with 10% chloral hydrate using intraperitoneal injection after 24 weeks.

Cell Culture^[14]

The lung tissue of neonatal Wistar rat (2 days after birth) was removed. Lung neonatal fibroblasts were isolated from the minced lung tissue using differential adhesion method and plated on 25 cm² plates in DMEM (BI-SH0019, BI, Kibbutz Beit-Haemek, Israel) containing 10% FBS (10099141, Gibco, Thermo Fisher Scientific) and 1% penicillin-streptomycin. Cells were cultured in a humidified atmosphere containing 5% CO₂ at 37 °C. Cells, at 80% confluence, were cultured in FBS-free DMEM for 24 h, when most cells were quiescent. Ang II (A-9525, Sigma, USA) was used to induce the differentiation of lung fibroblasts to myofibroblasts for 48 h. Fibroblasts were divided into four groups, 1) control; 2) Ang II (10^{-7} mol/L); 3) Ang II + Ang (1-7) (10^{-7} mol/L); 4) Ang II + Ang (1-7) + A779 (10^{-7} mol/L , H-2888, Bachem, USA).

Histopathological Observation

The right lower lung tissue was fixed in 4% neutral formalin solution for 48 h. The samples were sequentially dehydrated, embedded in paraffin, and cut into 4 μm thick sections. Hematoxylin and eosin

(H.E., BA4025, Baso Diagnostics Inc., Zhuhai, China) staining was used to observe lung fibrosis. Van Gieson (VG, BA4084, Baso Diagnostics Inc., Zhuhai, China) staining was used to assess collagen deposition. The number and size of silicotic nodules were evaluated by cellSens Dimension software (Olympus Corporation, Tokyo, Japan)^[15]. All sections (10 per group) were stained by H.E. and VG stains and three sections in different lung position from each sample were taken and analyzed.

Immunohistochemistry (IHC)

Antigen retrieval was performed using a high temperature and pressure method on dewaxed tissue sections and endogenous peroxidases were quenched using 0.3% H₂O₂. Samples were then incubated with primary antibodies against α -smooth muscle actin (α -SMA, 1:200, ab32575, Eptomics, Burlingame, CA) or ACE2 (1:200, sc-390851, Santa Cruz Biotechnology, Santa Cruz, CA) overnight at 4 °C, followed by incubation with secondary antibody (PV-6000, Beijing Zhongshan Jinqiao Biotechnology Co. Ltd, China) at 37 °C for 30 min. Immunoreactivity was visualized with DAB (ZLI-9018, ZSGB-BIO, Beijing, China). Brown staining was considered positive. Quantitative image analysis was conducted using Image-Pro Plus 6.1 software (Media Cybernetics, Inc., Rockville, MD, USA)^[16].

Immunofluorescence Staining

Neonatal rat fibroblasts were blocked with 10% donkey serum (92590, Temecula, CA, USA) for 30 min, and then, samples were co-incubated with α -SMA/ACE2 at 4 °C overnight. The samples were then incubated with the following products from Novex (Life Technologies, Frederick, MD, USA): donkey anti-rabbit IgG (H + L) TRITC (A16024, Molecular Probes, Carlsbad, CA, USA) and donkey anti-mouse IgG (H + L) FITC (A16016, Molecular Probes, Carlsbad, CA, USA) for 60 min at 37 °C. Nuclei were stained with DAPI (C1002, Beyotime Biological Technology Co. Ltd, Jiangsu, China). The cells were visualized using Olympus DP80 microscope and analyzed using imaging software (Olympus Soft Imaging).

Western Blot

The lung tissue and neonatal rat fibroblast lysates were extracted with RIPA buffer (BB-3201-1, BestBio, Shanghai, China) containing a protease inhibitor cocktail (Sigma-Aldrich). Protein

concentration in the supernatant was quantified using the Bradford protein assay (PC0020, Solarbio, Beijing, China). The proteins (20 μ g/lane) were separated by 10% SDS-polyacrylamide gel electrophoresis and were electro-transferred onto PVDF membranes. The membranes were then blocked with 5% non-fat milk and incubated overnight at 4 °C with primary antibody against collagen type I (Col I) (1:500, ab34710, Abcam, Cambridge, UK), α -SMA (1:500), ACE2 (1:500), Mas (1:500, AAR-013, Alomone Laboratories, Ltd., Jerusalem, Israel), and GAPDH (1:500, sc-25778, Santa Cruz). The membranes were then washed and incubated with 1:5000 diluted peroxidase-labeled affinity-purified antibodies to rabbit/mouse IgG (H + L) (074–1506/074–1806, Kirkegard and Perry Laboratories, Gaithersburg, MD, USA). Target bands were visualized by the addition of ECLTM Prime Western Blotting Detection Reagent (RPN2232, GE Healthcare). The results were normalized against GAPDH expression levels.

Enzyme-linked Immunosorbent Assay (ELISA)

Commercial ELISA kits were used to detect the content of Ang II (E04494r, CUSABIO Biotechnology Co. Ltd, China), Ang (1-7) (E14241r, CUSABIO Biotechnology Co. Ltd, China), and ACE2 (E14308r, CUSABIO Biotechnology Co. Ltd, China) in rat serum, according to the manufacturer's instructions. The level of each indicator in the serum was standardized with the protein concentration determined by Coomassie blue staining kit (Beyotime Biotechnology Co. Ltd, Shanghai, China).

Statistical Analysis

Statistical analysis was performed using SPSS 13.0 software. One-way ANOVA for multiple comparisons was used followed by post-hoc analysis with the Bonferroni test. Data were presented as mean \pm SEM. Differences with *P*-values < 0.05 were considered statistically significant.

RESULTS

Morphological Changes in the Rat Lung Tissue

H.E. and VG staining showed that the structure of alveoli was clear and alveolar wall was thin in control group. Cellular fibrous nodules were formed and high level of collagen was deposited in silicosis group. The number and size of silicotic nodules and collagen deposition decreased significantly in Ang

(1-7) treated group compared with silicosis group ($P < 0.05$, Figure 1).

Localization of α -SMA and ACE2 in the Rat Lung Tissue

IHC staining showed that α -SMA expressed in bronchial and vascular smooth muscle cell in control group. Positive expression of α -SMA was observed in silicotic nodules and fibrotic lesions in silicosis group and was decreased in Ang (1-7) treated group (Figure 2A, C). ACE2 expressed in bronchial epithelial cells and alveolar type II epithelial cells in control group. Expression of ACE2 was decreased in silicotic nodules and fibrosis lesions in silicosis group and increased after treatment with Ang (1-7) (Figure 2B, D).

Protein Expressions of Col I, α -SMA, ACE2, and Mas in the Rat Lung Tissue

Western blot indicated that the expression of Col I and α -SMA was increased in silicosis group and decreased after treatment with Ang (1-7). The expressions of ACE2 and Mas were decreased in

silicosis group and increased in Ang (1-7) treated group ($P < 0.05$, Figure 3A).

The Levels of ACE2, Ang (1-7), and Ang II in Rat Serum

ELISA indicated that the levels of ACE2 and Ang (1-7) in silicosis group were decreased significantly compared with control group. Ang (1-7) treated group exhibited increased expressions of ACE2 and Ang (1-7) compared with silicosis group ($P < 0.05$, Figure 3B, C). The expression level of Ang II was also detected, and the results showed that it was significantly increased in silicosis group and decreased after treatment with Ang (1-7) ($P < 0.05$, Figure 3D).

Localization and Expression of α -SMA and ACE2 in Neonatal Fibroblasts Detected by Immunofluorescence Staining

ACE2 was marked by FITC green fluorescence and α -SMA was marked by TRITC red fluorescence. The results indicated that α -SMA and ACE2 were expressed in cytoplasm of fibroblasts in control group.

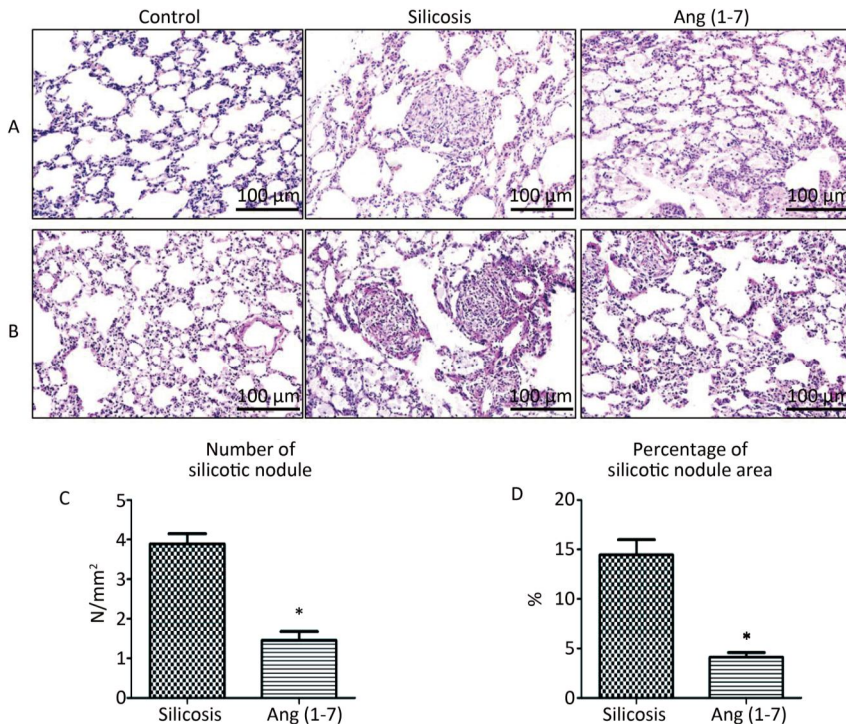


Figure 1. Formation of silicotic nodules and collagen deposition in the silicotic rat lung tissue. (A) HE staining. (B) VG staining. Scale bars = 100 μ m. (C, D) Quantitative assessment of silicotic nodules' number and area in the lungs of silicosis and Ang (1-7) treated groups. Data are expressed as mean \pm SE. * $P < 0.05$ as compared with silicosis group ($n = 10$, rats).

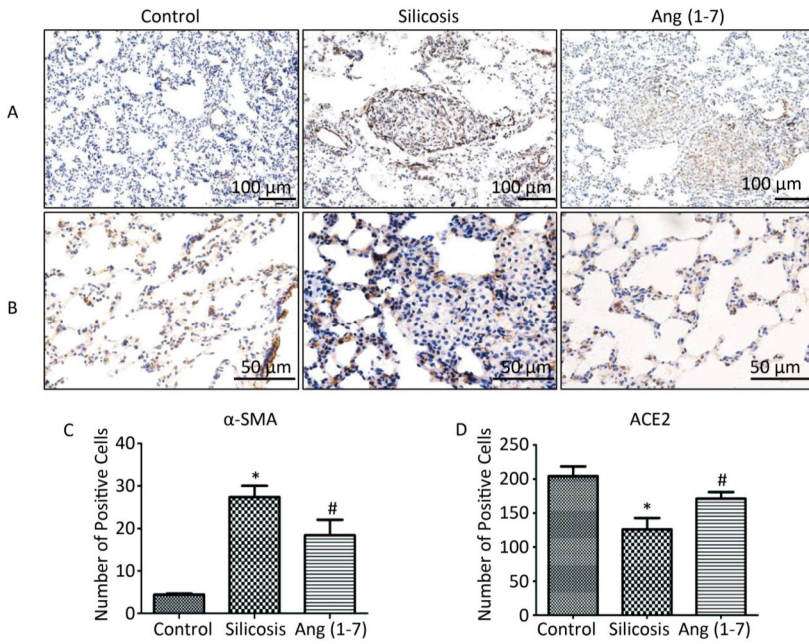


Figure 2. Effect of Ang (1-7) on expressions of α-SMA and ACE2 in the silicotic rat lung tissue observed by IHC. (A) α-SMA, Scale bars = 100 μm. (B) ACE2, Scale bars = 50 μm. (C) The number of α-SMA-positive cells in the lung. (D) The number of ACE2-positive cells in the lung. Data are expressed as mean ± SE. *P < 0.05 as compared with control group; #P < 0.05 as compared with silicosis group (n = 10, rats).

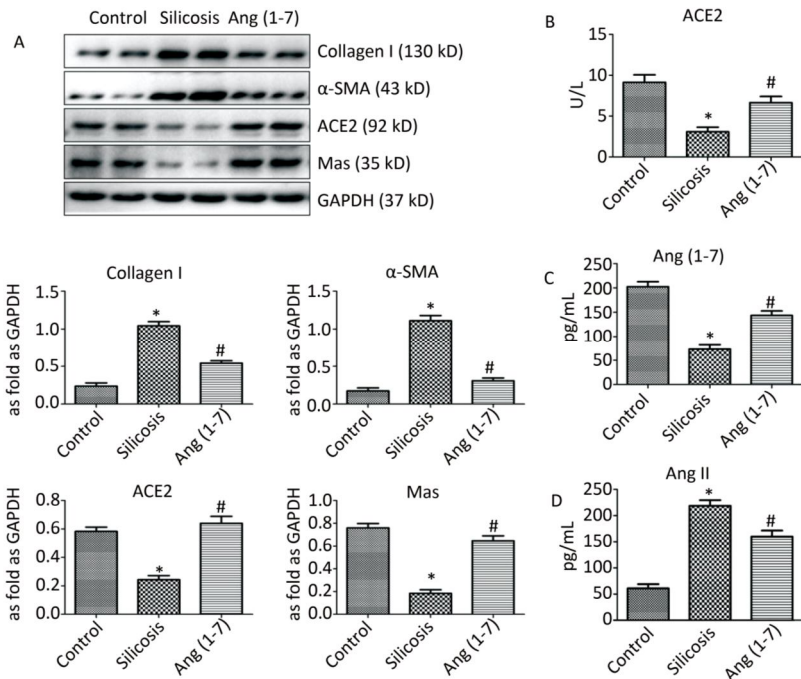


Figure 3. (A) Effect of Ang (1-7) treatment on the protein expressions of Col I, α-SMA, ACE2, and Mas in the silicotic rat lung tissue evaluated by Western blot. The results were normalized with GAPDH levels. Data are expressed as mean ± SE. *P < 0.05 as compared with control group; #P < 0.05 as compared with silicosis group (n = 4, samples *in vitro*). Levels of ACE2, Ang (1-7), and Ang II in rat serum measured by ELISA. (B) ACE2 (C) Ang (1-7) (D) Ang II. Data are expressed as mean ± SE, *P < 0.05 as compared with control group; #P < 0.05 as compared with silicosis group (n = 10, rats).

The fluorescence of α -SMA and ACE2 enhanced and decreased, respectively, when stimulated by Ang II. Treatment with Ang (1-7) decreased the fluorescence of α -SMA and increased the fluorescence of ACE2 compared with Ang II group. The effect of Ang (1-7) was suppressed after treatment with A779 (Figure 4).

Protein Expressions of Col I, α -SMA, ACE2, and Mas in Neonatal Fibroblasts

Western blot showed upregulation of Col I and α -SMA in Ang II group and treatment with Ang (1-7) decreased the expressions of Col I and α -SMA. Compared with control group, the expressions of ACE2 and Mas were downregulated when stimulated by Ang II and upregulated after treatment with Ang (1-7). The results also indicated that the protein expressions of Col I and α -SMA were increased and those of ACE2 and Mas were decreased after treatment with A779 compared with Ang (1-7) treated group ($P < 0.05$, Figure 5).

DISCUSSION

In this study, we demonstrated that ACE2-Ang (1-7)-Mas axis was involved in silica-induced pulmonary fibrosis and provided new evidence for the anti-silicosis strategy of using Ang (1-7).

Silicosis is mainly caused by long-term inhalation of silica dust in occupational environment, which induces the formation of silicotic nodules and pulmonary fibrosis. In the present study, the experimental rat silicosis model

was established by HOPE-MED 8050 exposure control apparatus, which resembled human silicosis model. To observe the interstitial fibrosis and detect the collagen deposition in the lung, we first observed and analyzed the lung histopathological changes using HE and VG staining. The results indicated that fibrous-cellular silicotic nodules with diffuse interstitial fibrosis and collagen deposition were observed in silicosis group. Number and size of silicotic nodules were also evaluated and the results showed they were increased significantly in silicotic rats compared with control group. Myofibroblasts, expressing α -SMA^[17,18], are generated from epithelia or fibroblasts and play an important role in progression of fibrotic diseases. Therefore, the IHC profiles of α -SMA were observed in order to identify their location in the silicotic lung. IHC revealed that α -SMA-expressing myofibroblasts were distributed in silicotic nodules and interstitial fibrotic lesions in silicosis group. Further characterization with Western blot demonstrated that the expressions of Col I and α -SMA were significantly increased in silicosis group and fibroblasts stimulated by Ang II. These results suggested that silicosis model and myofibroblast differentiation model were successfully established.

In contrast to the fibrogenic and proliferative actions of the ACE-Ang II-AT1 axis, it has been suggested that the ACE2-Ang (1-7)-Mas axis exhibits anti-fibrogenic and anti-proliferative activities^[19]. Experimental studies indicated that ACE2 and Ang (1-7) exhibit beneficial effects on lung injury^[20]

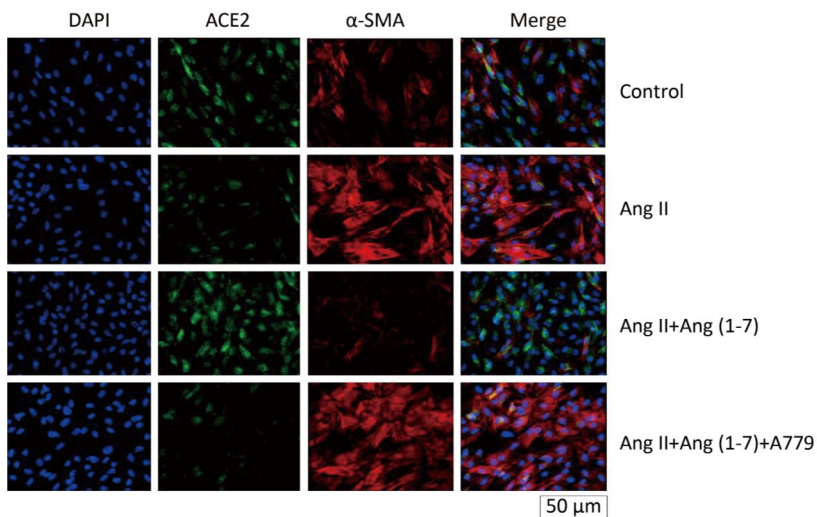


Figure 4. Effect of Ang (1-7) on co-expression of α -SMA and ACE2 in neonatal fibroblast observed by immunofluorescence staining. Scale bars = 50 μ m.

and ACE2 could protect against bleomycin-induced fibrosis^[12]. In the present study, we hypothesized that ACE2-Ang (1-7)-Mas axis participated in the progression of silicosis and treatment with Ang (1-7) had protective effect on silicotic fibrosis. H.E. and VG staining indicated that the number and size of silicotic nodules and collagen deposition were significantly decreased in Ang (1-7) treated group compared with silicosis group. Ang (1-7) treatment also decreased the expressions of Col I and α -SMA in the silicotic lung tissue and fibroblasts induced by Ang II as detected by IHC and Western blot. These results indicated Ang (1-7) had beneficial effects on silicosis. ACE2 is normally expressed in vascular endothelial cell, alveolar epithelial cell, and bronchial epithelial cell, and exhibits protective effect on pulmonary fibrosis^[21]. In the present study, IHC staining showed that the ACE2 expression decreased in silicotic nodule which indicated the apoptosis of alveolar epithelial cells in silicotic nodule, whereas Ang (1-7) treatment increased the expression of ACE2 compared with silicosis group. Western blotting also demonstrated that the expressions of ACE2 and Mas

were decreased in silicosis group and fibroblasts induced by Ang II and Ang (1-7) increased the expressions of ACE2 and Mas. Ang (1-7), a heptapeptide converted from Ang II under catalytic action of ACE2, binds to a distinct plasma membrane G protein coupled receptor, the Mas receptor, and exhibits anti-fibrotic, anti-proliferative and anti-inflammatory effects. A recent study demonstrated that long-term AT2 receptor activation increased renal ACE2 activity, and exogenous Ang (1-7) treatment significantly increased myocardial ACE2 activity and Ang (1-9) level, possibly *via* its effect on AT2, and that activated ACE2 may catalyze Ang II into Ang (1-7), thus forming a positive feedback^[22,23]. Our results also indicated that Ang (1-7) regulated the expressions of ACE2 and Mas. ELISA was used to observe the circular RAS and the results indicated that the levels of ACE2 and Ang (1-7) were decreased in silicotic rat serum and treatment with Ang (1-7) increased the levels of ACE2 and Ang (1-7). In addition, Ang (1-7) decreased Ang II level in rat serum. A779, a Mas receptor inhibitor, was also used

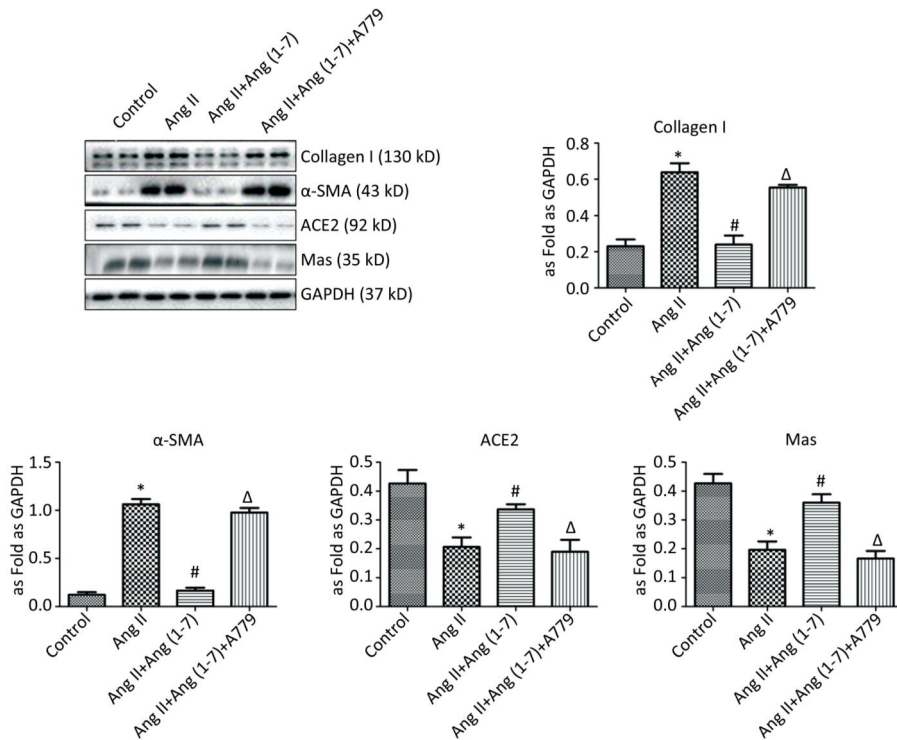


Figure 5. Effect of Ang (1-7) on protein expressions of Col I, α -SMA, ACE2, and Mas in neonatal fibroblasts measured by Western blot. The results were normalized with GAPDH levels. Data are expressed as mean \pm SE. * $P < 0.05$ as compared with control group; # $P < 0.05$ as compared with Ang II group; $\Delta P < 0.05$ as compared with Ang (1-7) group ($n = 4$, samples *in vitro*).

in the study to explore the protective effect of Ang (1-7) on myofibroblast differentiation induced by Ang II. Immunofluorescence staining indicated that the fluorescence of ACE2 decreased and of α -SMA enhanced after treatment with A779 compared with Ang (1-7) group. Western blot also demonstrated that the expressions of ACE2 and Mas were downregulated, and expressions of Col I and α -SMA were upregulated in A779 treated group. These findings revealed that ACE2-Ang (1-7)-Mas axis participates in the pathogenesis of silicosis and Ang (1-7) enhanced the silicosis and myofibroblast differentiation stimulated by Ang II *via* Mas receptor.

CONCLUSION

In summary, the present study suggested that Ang (1-7) modulated ACE2-Ang (1-7)-Mas axis to promote silicosis and myofibroblast differentiation stimulated by Ang II.

COMPETING INTERESTS

The authors declare that there is no competing interest.

AUTHORS' CONTRIBUTIONS

ZHANG Bo Nan and XU Hong designed the study and drafted the manuscript. GAO Xue Min, ZHANG Gui Zhen, and ZHANG Xin carried out the experimental work and analyzed the data. YANG Fang participated in the design of the study and critically reviewed the manuscript and provided intellectual input. All authors read and approved the final version of manuscript.

Received: December 26, 2018;

Accepted: April 10, 2019

REFERENCES

1. Stanbury M, Rosenman KD. Occupational health disparities: a state public health based approach. *Am J Ind Med*, 2014; 57, 596-604.
2. Leung C, Yu I, Chen W. Silicosis. *Lancet*, 2012; 379, 2008-18.
3. Rimal B, Greenberg AK, Rom WN. Basic pathogenetic mechanisms in silicosis: current understanding. *Curr Opin Pulm Med*, 2005; 11, 169-73.
4. Wang J, Chen L, Chen B, et al. Chronic Activation of the Renin-Angiotensin System Induces Lung Fibrosis. *Sci Rep*, 2015; 5, 15561.
5. Murphy AM, Wong AL, Bezuhy M. Modulation of angiotensin II signaling in the prevention of fibrosis. *Fibrogenesis Tissue Repair*, 2015; 8, 7.
6. Wang M, Chen DQ, Chen L, et al. Novel inhibitors of the cellular RAS components, Poricoic acids, target Smad3 phosphorylation and Wnt/ β -catenin pathway against renal fibrosis. *Br J Pharmacol*, 2018; 175, 2689-708.
7. Chen H, Yang T, Wang MC, et al. Novel RAS inhibitor 25-O-methylalisol F attenuates epithelial-to-mesenchymal transition and tubulo-interstitial fibrosis by selectively inhibiting TGF- β -mediated Smad3 phosphorylation. *Phytomedicine*, 2018; 42, 207-18.
8. Zielonka TM, Zycinska K, Chorostowska-Wynimko J, et al. Angiogenic activity of sera from interstitial lung disease patients in relation to angiotensin-converting enzyme activity. *Adv Exp Med Biol*, 2013; 756, 213-21.
9. Xu H, Yang F, Sun Y, et al. A new antifibrotic target of Ac-SDKP: inhibition of myofibroblast differentiation in rat lung with silicosis. *PLoS One*, 2012; 7, e40301.
10. Uhal BD, Li X, Piasecki CC, et al. Angiotensin signalling in pulmonary fibrosis. *Int J Biochem Cell Biol*, 2012; 44, 465-8.
11. Fraga-Silva RA, Ferreira AJ, Dos Santos RA. Opportunities for targeting the angiotensin-converting enzyme 2/angiotensin-(1-7)/Mas receptor pathway in hypertension. *Curr Hypertens Rep*, 2013; 15, 31-8.
12. Meng Y, Yu CH, Li W, et al. Angiotensin-Converting Enzyme 2/Angiotensin-(1-7)/Mas Axis Protects against Lung Fibrosis by Inhibiting the MAPK/NF- κ B Pathway. *Am J Respir Cell Mol Biol*, 2014; 50, 723-36.
13. Chang Seong Kim, In Jin Kim, Eun Hui Bae, et al. Angiotensin-(1-7) Attenuates Kidney Injury Due to Obstructive Nephropathy in Rats. *PLoS One*, 2015; 10, e0142664.
14. Xie H, Lu J, Zhu Y, et al. The KCa3.1 blocker TRAM-34 inhibits proliferation of fibroblasts in paraquat-induced pulmonary fibrosis. *Toxicol Letters*, 2018; 295, 408-15.
15. Liu Y, Xu H, Geng YC, et al. Dibutyl-*c*-AMP attenuates pulmonary fibrosis by blocking myofibroblast differentiation via PKA/CREB/CBP signaling in rats with silicosis. *Respir Res*, 2017; 18, 38.
16. Wang CJ, Zhou ZG, Holmqvist A, et al. Survivin expression quantified by Image Pro-Plus compared with visual assessment. *Appl Immunohistochem Mol Morphol*, 2009; 17, 530-5.
17. Zhou B, Liu Y, Kahn M, et al. Interactions between beta-catenin and transforming growth factor-beta signaling pathways mediate epithelial-mesenchymal transition and are dependent on the transcriptional co-activator cAMP-response element-binding protein (CREB)-binding protein (CBP). *J Biol Chem*, 2012; 287, 7026-38.
18. Tumelty KE, Smith BD, Nugent MA, et al. Aortic carboxypeptidase-like protein (ACLP) enhances lung myofibroblast differentiation through transforming growth factor beta receptor-dependent and -independent pathways. *J Biol Chem*, 2014; 289, 2526-36.
19. Ferrario CM. ACE2: more of Ang-(1-7) or less AngII? *Curr Opin Nephrol Hypertens*, 2011; 20, 1-6.
20. Santos RA, Ferreira AJ, Verano-Braga T, et al. Angiotensin-converting enzyme 2, angiotensin-(1-7) and Mas: new players of the renin-angiotensin system. *J Endocrinol*, 2013; 216, R1-17.
21. VinayakShenoy, Qi YF, Michael J Katovich. ACE2, a Promising Therapeutic Target for Pulmonary Hypertension. *Curr Opin Pharmacol*, 2011; 11, 150-5.
22. Ali Q, Wu Y, Hussain T. Chronic AT2 receptor activation increases renal ACE2 activity, attenuates AT1 receptor function and blood pressure in obese Zucker rats. *Kidney Int*, 2013; 84, 931-9.
23. Hao PP, Yang JM, Liu YP, et al. Combination of angiotensin-(1-7) with perindopril is better than single therapy in ameliorating diabetic cardiomyopathy. *Sci Rep*, 2015; 5, 8794.